Available online at www.sciencedirect.com
ScienceDirect
Energy Procedia 00 (2011) 1–10
Energy Procedia
www.elsevier.com/locate/procedia

6th Trondheim CCS Conference

Two-Phase Flow of CO_2 with Phase Transfer

Halvor Lund[a,*], Peder Aursand[b]

[a] *Dept. of Energy and Process Engineering, Norwegian University of Science and Technology (NTNU), NO-7491 Trondheim, Norway*
[b] *SINTEF Energy Research, Sem Sælands vei 11, NO-7465 Trondheim, Norway*

Abstract

A model for two-phase pipeline flow of CO_2 with phase transfer is presented. Two different relaxation models for phase transfer are developed. The system of equations is solved by splitting it into a hyperbolic conservation law and a relaxation ODE, solved by a multi-stage (MUSTA) finite volume scheme and the backward Euler method, respectively. The stiffened-gas equation of state is used for calculating thermodynamic properties. Simulation results from a depressurisation case of a CO_2 pipe, causing phase change and cooling, are presented, showing that statistical rate theory predicts solutions close to those of an equilibrium model with instant phase transfer.

Keywords: Evaporation, condensation, phase transfer, two-phase, pipeline
PACS: 64.70.fm, 47.40.-x, 47.55.-t
2010 MSC: 35L40, 35L60, 35Q35

1. Introduction

Carbon dioxide capture and storage (CCS) will potentially be an important contributor to mitigating emission of CO_2 from stationary sources. In the BLUE map of the International Energy Agency (IEA) [1], CCS accounts for 19% of CO_2 emission reductions in 2050. Transport from the point of capture to a storage site is a necessary part of a CCS system and may take place using e.g. ships or pipelines. Experience with multi-phase flow in pipelines is abundant in the oil and gas industry as well as in the nuclear industry. However, knowledge on two-phase flow of CO_2 is available to a lesser extent.

Transport of CO_2 will typically take place at high pressure, at conditions at which the CO_2 is in its supercritical phase. However, during a pressurisation from atmospheric pressure or during a planned or possibly uncontrolled depressurisation, the fluid may enter the two-phase region with gas and liquid coexisting. Due to phase change in such a situation, the fluid will cool significantly, potentially leading to temperatures low enough to make the pipe steel brittle. This, in turn, makes the pipe vulnerable to rupture and possible severe damage. The prediction of the temperature drop during such depressurisations requires modeling of phase transfer (i.e. evaporation and condensation) between the two phases.

*Corresponding author
Email address: halvor.lund@ntnu.no (Halvor Lund)

Our paper is organized as follows: In Section 2, we present our two-phase drift-flux flow model, which needs a phase transfer model to be fully defined. Two such models are developed in Section 3. Section 4 briefly describes the thermodynamic model (equation of state) we have used. The numerical methods used to solve the fluid-mechanical and phase transfer equations are presented in Section 5. Results from a depressurisation of a CO_2 pipeline are presented in Section 6. Finally, Section 7 concludes our work.

2. Two-phase flow model

The goal of our work is to demonstrate modeling of a phase transfer process in a pipe with two-phase flow. We therefore aim for a model which incorporates phase transfer, but otherwise is as simple as possible. Hence, we make the assumptions that the two phases

1. have equal velocities, i.e. a homogeneous flow model,
2. are in thermal equilibrium, i.e. have equal temperatures,
3. are in mechanical equilibrium, i.e. have equal pressures.

This allows us to formulate a four-equation drift-flux model consisting of two mass balance equations, and conservation equations for the total momentum and energy.

$$\frac{\partial(\alpha_{\mathrm{g}}\rho_{\mathrm{g}})}{\partial t} + \frac{\partial(\alpha_{\mathrm{g}}\rho_{\mathrm{g}}v)}{\partial x} = \Gamma, \tag{1}$$

$$\frac{\partial(\alpha_{\ell}\rho_{\ell})}{\partial t} + \frac{\partial(\alpha_{\ell}\rho_{\ell}v)}{\partial x} = -\Gamma, \tag{2}$$

$$\frac{\partial(\rho v)}{\partial t} + \frac{\partial(\rho v^2 + p)}{\partial x} = 0, \tag{3}$$

$$\frac{\partial E}{\partial t} + \frac{\partial[(E + p)v]}{\partial x} = 0, \tag{4}$$

where α_k is the volume fraction of phase k, ρ_k is the density of phase k, and $\rho = \alpha_{\mathrm{g}}\rho_{\mathrm{g}} + \alpha_{\ell}\rho_{\ell}$ is the mixture density. The fluid velocity is denoted by v and the pressure by p. The total energy per unit volume, E, is given by

$$E = E_{\mathrm{g}} + E_{\ell}, \tag{5}$$

$$E_k = \alpha_k\rho_k(e_k + \frac{1}{2}v^2), \quad k \in \{\mathrm{g}, \ell\}, \tag{6}$$

where e_k is the internal energy per mass of phase k. The phase transfer source term appears in the mass balance equations as Γ. This model has been analyzed by e.g. Flåtten and Lund [2] and Flåtten, Morin, and Munkejord [3] in the non-stiff limit where $\Gamma \to 0$.

The two-phase flow model presented above has the advantage of being quite simple, while still allowing for phase transfer modeling; the only simpler alternative possibly being an isentropic model. Although terms accounting for e.g. wall friction, heat transfer between the pipe and the fluid, and fluid heat conduction are omitted here, such terms may be added later if desired.

3. Phase transfer model

The phase transfer can be written (disregarding the transport terms) as

$$\frac{\mathrm{d}(\alpha_{\mathrm{g}}\rho_{\mathrm{g}})}{\mathrm{d}t} = -\frac{\mathrm{d}(\alpha_{\ell}\rho_{\ell})}{\mathrm{d}t} = \Gamma. \tag{7}$$

Physically, differences in the chemical potentials of the two phases will cause a mass flux from one phase to the other, in the direction of decreasing chemical potential. We therefore seek a phase transfer term in the form

$$\Gamma = \mathcal{K}(\mu_{\ell} - \mu_{\mathrm{g}}), \tag{8}$$

where $\mathcal{K} > 0$ is some function of flow and thermodynamic variables. The function $\mathcal{K}$ should fulfill some important requirements:

1. $\mathcal{K} = 0$ if $m_\mathrm{g} = 0$ and $\mu_\mathrm{g} > \mu_\ell$
2. $\mathcal{K} = 0$ if $m_\ell = 0$ and $\mu_\mathrm{g} < \mu_\ell$

These requirements avoids phase transfer *from* a non-existing phase.

In the limit where $\mathcal{K} \to \infty$, we arrive at an equilibrium model in which phase transfer is instantaneous, i.e. the phases always have equal chemical potential. In this limit, the model (1)–(4) may be written as the classical Euler equations of gas dynamics [2],

$$\frac{\partial \rho}{\partial t} + \frac{\partial (\rho v)}{\partial x} = 0, \qquad \frac{\partial (\rho v)}{\partial t} + \frac{\partial (\rho v^2 + p)}{\partial x} = 0, \qquad \frac{\partial E}{\partial t} + \frac{\partial [(E + p)v]}{\partial x} = 0. \tag{9}$$

This model is also known as the homogeneous equilibrium model, which was investigated for use in carbon dioxide pipeline depressurisation simulations in Ref. [4].

3.1. Simple model

As an initial approach, we suggest the simplest model possible which fulfills the two requirements stated earlier,

$$\mathcal{K} = \begin{cases} \mathcal{K}_0 m_\mathrm{g} & \text{if } \mu_\mathrm{g} > \mu_\ell, \\ \mathcal{K}_0 m_\ell & \text{if } \mu_\mathrm{g} < \mu_\ell, \\ 0 & \text{otherwise,} \end{cases} \tag{10}$$

where $\mathcal{K}_0 > 0$ is an adjustable parameter whose magnitude determines the rate of the phase transfer. The value of $\mathcal{K}_0$ in this model is unknown, which makes it more of a qualitative model. We would like to compare it with a quantitative model, in which the magnitude of $\mathcal{K}$ is more precise. To this end, we develop an expression based on statistical rate theory in the following section.

3.2. Statistical rate theory

In the literature, modeling of mass fluxes across interfaces is described using a variety of different approaches. Of the most common are kinetic theory and irreversible (non-equilibrium) thermodynamics. Recently, statistical rate theory (SRT) has been proposed by Ward and Fang [5] as an alternative approach to model liquid evaporation. One of the reasons of the introduction of SRT was that kinetic theory predicted unreasonable temperature profiles near the interface [6], so-called anomalous temperature profiles. Further discussion on this matter can be found in the works of Koffman, Plesset, and Lees [7] and Rahimi and Ward [8]. The SRT model predicts more reasonable temperature profiles, in better accordance with experimental results. Another significant advantage of SRT when modeling evaporation and condensation, compared to kinetic theory or irreversible thermodynamics, is that it is free of any fitting parameters.

Statistical rate theory is a rather new approach to modeling of evaporation and condensation, based on transition probabilities from quantum mechanics and the Boltzmann definition of entropy. It assumes that the interfacial transport processes are the result of single molecular events and calculates the probabilities using first-order perturbation analysis of the Schrödinger equation. The theory was first introduced by Ward [9] in 1977, and was later laid out more fundamentally in the early 1980s by Ward, Findlay, and Rizk [10]. It has since been applied to as diverse transport processes as crystal growth [11], solution/solid adsorption [12, 13], gas/solid adsorption [14, 15], temperature programmed desorption [16], ion permeation across lipid membranes [17], chemical reactions [18], and evaporation and condensation [5, 19, 20].

We will now derive an expression for the evaporation and condensation mass flux, based on the SRT model, closely following the derivations in Refs. [5, 10]. As noted previously, the SRT approach is based on the probability of single molecular events. Let λ_j denote a "current" molecular distribution, and λ_k denote a distribution in which one molecule has been transferred from the liquid phase to the vapor. From perturbation analysis, the probability of a transition from distribution λ_j to λ_k is [10]

$$\tau(\lambda_j \to \lambda_k) = K(\lambda_j \to \lambda_k) \frac{\Omega(\lambda_k)}{\Omega(\lambda_j)}, \tag{11}$$

where $\Omega(\lambda)$ is the number of microscopic states with molecular distribution λ. The constant K will be determined later in the derivation. Using the Boltzmann definition of entropy, the probability (11) reads

$$\tau(\lambda_j \to \lambda_k) = K(\lambda_j \to \lambda_k) \exp\left[\frac{S(\lambda_k) - S(\lambda_j)}{k_B}\right], \tag{12}$$

where $S(\lambda)$ is the total entropy of the molecular distribution λ. Similarly, let λ_i denote a distribution in which one molecule has been transferred from the vapor phase to the liquid. The probability for this transition, $\tau(\lambda_j \to \lambda_i)$, is then given by Eq. (12) with k replaced by i. The change in entropy from one state to the other is given by the sum over all phases. The change of entropy can then be expressed as

$$S(\lambda_k) - S(\lambda_j) = \sum_{i=\mathrm{g},\ell} (S_i(\lambda_k) - S_i(\lambda_j)) = \sum_{i=\mathrm{g},\ell} \Delta S_i, \tag{13}$$

where $\Delta S_i \equiv S_i(\lambda_k) - S_i(\lambda_j)$ is the change in entropy of phase i. From the Gibbs-Duhem relation and the fundamental relation $U = TS - pV + gN$, we have [10]

$$T_i \Delta S_i = \Delta U_i + p_i \Delta V_i - g_i \Delta N_i, \tag{14}$$

where g_i is the chemical potential per molecule, U_i is the total internal energy, T_i is the temperature and N_i the number of molecules in phase i. Solving for ΔS_i and inserting into the sum in Eq. (13) yields

$$S(\lambda_k) - S(\lambda_j) = \frac{\Delta U_\mathrm{g} + p_\mathrm{g} \Delta V_\mathrm{g} - g_\mathrm{g} \Delta N_\mathrm{g}}{T_\mathrm{g}} + \frac{\Delta U_\ell + p_\ell \Delta V_\ell - g_\ell \Delta N_\ell}{T_\ell}. \tag{15}$$

We recall that the transition from distribution λ_j to λ_k corresponds to one molecule making the transition from the liquid to the gas phase, which means that $\Delta N_\ell = -1$ and $\Delta N_\mathrm{g} = 1$. We can also utilize that the phases have equal pressures and temperatures (by definition in our model), which yields

$$S(\lambda_k) - S(\lambda_j) = \frac{1}{T}(\Delta U_\mathrm{g} + \Delta U_\ell + p(\Delta V_\mathrm{g} + \Delta V_\ell) + g_\ell - g_\mathrm{g}). \tag{16}$$

Since we are considering an isolated system, the total energy and total volume are conserved, thus we have

$$S(\lambda_k) - S(\lambda_j) = \frac{1}{T}(g_\ell - g_\mathrm{g}). \tag{17}$$

The chemical potential per mass, μ_k, can easily be calculated by dividing g_k by the molecule mass. We may now insert the entropy expressions in the expression for the transition probability (12), yielding

$$\tau(\lambda_j \to \lambda_k) = K_{\ell \to \mathrm{g}} \exp\left[\frac{1}{k_B T}(g_\ell - g_\mathrm{g})\right] \tag{18}$$

for the transport from liquid to gas, where we write $K_{\ell \to \mathrm{g}} \equiv K(\lambda_j \to \lambda_k)$ to make the direction liquid-to-gas clearer. Similarly, for transport from gas to liquid we get

$$\tau(\lambda_j \to \lambda_i) = K_{\mathrm{g} \to \ell} \exp\left[\frac{1}{k_B T}(g_\mathrm{g} - g_\ell)\right]. \tag{19}$$

The number of molecules transferred from liquid to gas in a time Δt is

$$\Delta N_{\ell \to \mathrm{g}} = \tau(\lambda_j \to \lambda_k) \Delta t, \tag{20}$$

provided that Δt is small enough not to change τ. The flux (number of transitions per time per area) is then

$$j_{\ell \to \mathrm{g}} = \frac{\Delta N_{\ell \to \mathrm{g}}}{\Delta t} = K_{\ell \to \mathrm{g}} \exp\left[\frac{1}{k_B T}(g_\ell - g_\mathrm{g})\right]. \tag{21}$$

An equivalent expression applies to the transition from gas to liquid. This is equivalent to the expression which Ward and Fang [5] arrive at, if one assumes equal temperatures.

The net flux from liquid to gas can then be written as the difference between the fluxes in each direction, yielding the net flux

$$j = j_{\ell\to \mathrm{g}} - j_{\mathrm{g}\to\ell} = K_{\ell\to \mathrm{g}} \exp\left[\frac{1}{k_B T}(g_\ell - g_{\mathrm{g}})\right] - K_{\mathrm{g}\to\ell} \exp\left[\frac{1}{k_B T}(g_{\mathrm{g}} - g_\ell)\right] \tag{22}$$

In an equilibrium condition, with $g_{\mathrm{g}} = g_\ell$, the two fluxes have to cancel each other, giving a net flux of zero. This means that $K_{\ell\to \mathrm{g}} = K_{\mathrm{g}\to\ell} = K_e$. To calculate the value of this constant, we turn to classical kinetic theory and assume that in equilibrium all molecules that collide with the liquid-vapor interface are transferred to the other phase. The collision rate of gas molecules can be predicted using the Maxwell-Boltzmann velocity distribution, and may be expressed as

$$K_e = \rho_{\mathrm{g}} \sqrt{\frac{k_B T}{2\pi m^3}}, \tag{23}$$

where m is the molecular mass. This is a well-known result for ideal gases, but as Kapoor and Elliott [19] point out, it is equally valid for a non-ideal gas. Furthermore, we assume that we always are close to equilibrium, so that we always have $K_e = K_{\ell\to \mathrm{g}} = K_{\mathrm{g}\to\ell}$. We may now write the mass flux, obtained by multiplying the net flux (22) by the molecular mass m, as

$$J = \rho_{\mathrm{g}} \sqrt{\frac{kT}{2\pi m}} \left(\exp\left[\frac{g_\ell - g_{\mathrm{g}}}{k_B T}\right] - \exp\left[\frac{g_{\mathrm{g}} - g_\ell}{k_B T}\right]\right). \tag{24}$$

This expression is, as we can see, free of any fitting parameters.

Having a flux, we only need an expression for the interfacial area to arrive at an expression for the transferred mass Γ. First, we express the total gas mass M_{g} in a pipe section of length ΔL as

$$M_{\mathrm{g}} = \rho_{\mathrm{g}} A_{\mathrm{g}} \Delta L = \alpha_{\mathrm{g}} \rho_{\mathrm{g}} A \Delta L, \tag{25}$$

where A_{g} is the area of the pipe cross section occupied by gas. The time derivative of this quantity is caused by the flux across the interface,

$$\frac{\mathrm{d}M_{\mathrm{g}}}{\mathrm{d}t} = J A_{\mathrm{int}} = J W_{\mathrm{int}} \Delta L \tag{26}$$

where A_{int} is the interfacial area in the pipe section, and W_{int} is the width of the interface across the pipe cross-section. By differentiating Eq. (25) with respect to time and using Eq. (7), we get

$$\frac{\mathrm{d}M_{\mathrm{g}}}{\mathrm{d}t} = \frac{\mathrm{d}(\alpha_{\mathrm{g}} \rho_{\mathrm{g}})}{\mathrm{d}t} A \Delta L = \Gamma A \Delta L. \tag{27}$$

The two last equations yield

$$\Gamma = \frac{4 J W_{\mathrm{int}}}{\pi D^2}, \tag{28}$$

where we have used that the cross-sectional area of a circular pipe with diameter D is $A = \pi D^2/4$.

When it comes to approximating the interface width W_{int}, a number of considerations have to be made. We wish it to be zero when no mass is left in the *source* phase, but greater than zero when there is no mass in the *receiving* phase. The latter is necessary to allow a start-up of the condensation or evaporation process, even without presence of the phase which receives mass . We may then suggest

$$W_{\mathrm{int}} = \begin{cases} 4D(\alpha_{\mathrm{g}} + \delta)\alpha_\ell & \text{if } g_{\mathrm{g}} < g_\ell, \\ 4D\alpha_{\mathrm{g}}(\alpha_\ell + \delta) & \text{if } g_\ell < g_{\mathrm{g}}, \\ 0 & \text{otherwise,} \end{cases} \tag{29}$$

where $\delta \ll 1$ is a tunable *initial volume fraction*, to avoid zero interfacial area when one phase disappears. This factor will only govern the start-up phase of evaporation or condensation, when the volume fraction α_k of the receiving phase is on the order of δ. W_{int} may be looked upon as an approximation of the interfacial width in stratified flow, with $W_{\text{int}}(\alpha_{\text{g}} = 0.5) = D + O(\delta)$. Almost all other flow regimes will have a larger interface width.

Inserting the expressions for J and W_{int} from Eqs. (24) and (29) into Eq. (28) yields

$$\Gamma = \begin{cases} \frac{16\rho_{\text{g}}(\alpha_{\text{g}}+\delta)\alpha_\ell}{\pi D}\sqrt{\frac{k_B T}{2\pi m}}\left(\exp\left[\frac{m(\mu_\ell-\mu_{\text{g}})}{k_B T}\right] - \exp\left[\frac{m(\mu_{\text{g}}-\mu_\ell)}{k_B T}\right]\right) & \text{if } \mu_{\text{g}} < \mu_\ell, \\ \frac{16\rho_{\text{g}}\alpha_{\text{g}}(\alpha_\ell+\delta)}{\pi D}\sqrt{\frac{k_B T}{2\pi m}}\left(\exp\left[\frac{m(\mu_\ell-\mu_{\text{g}})}{k_B T}\right] - \exp\left[\frac{m(\mu_{\text{g}}-\mu_\ell)}{k_B T}\right]\right) & \text{if } \mu_\ell \leq \mu_{\text{g}}, \end{cases} \tag{30}$$

where we have used that $g_k = m\mu_k$ and μ_k is the chemical potential per mass for phase k. Bond [21] notes that the exponents in (30) are small enough to allow a linearizing of the exponential terms. Expanding (30) in powers of $\Delta\mu = \mu_\ell - \mu_{\text{g}}$ then yields

$$\Gamma = \begin{cases} \frac{32\rho_{\text{g}}(\alpha_{\text{g}}+\delta)\alpha_\ell}{\pi D}\sqrt{\frac{m}{2\pi k_B T}}(\mu_\ell - \mu_{\text{g}}) & \text{if } \mu_{\text{g}} < \mu_\ell, \\ \frac{32\rho_{\text{g}}\alpha_{\text{g}}(\alpha_\ell+\delta)}{\pi D}\sqrt{\frac{m}{2\pi k_B T}}(\mu_\ell - \mu_{\text{g}}) & \text{if } \mu_\ell \leq \mu_{\text{g}}. \end{cases} \tag{31}$$

In this form, the phase transfer process may be viewed as a relaxation of the difference in chemical potential, $\Delta\mu \equiv \mu_\ell - \mu_{\text{g}}$. Other authors, e.g. Saurel et al. [22] and Stewart and Wendroff [23], have discussed phase transfer models in this form, however without giving an explicit expression for the rate constant, which we have managed to obtain here. The two-phase flow models presented by Bestion [24], Chung et al. [25], Cortes [26], and Toumi [27] also include mass transfer models in different forms, but Toumi [27] points out that his model is not chosen for its physical validity, but rather for its simplicity. We would like to point out the advantage of our model having both a physical basis and an explicit mathematical expression.

4. Equation of state

We choose to use the *stiffened gas* equation of state (EOS), advocated by e.g. Menikoff [28, 29], as our thermodynamic model. The stiffened-gas EOS can be seen as a local linearisation of a more general EOS, and is mathematically similar to the ideal gas EOS, but with stiffening terms to allow for finite density at zero pressure. It has the important advantage of being significantly simpler than most other EOSes, while still being relatively accurate in the vicinity of a chosen reference point.

The pressure, internal energy and chemical potential (for a single phase) are given by

$$p(\rho, T) = \rho(\gamma - 1)c_v T - p_\infty, \tag{32}$$

$$e(\rho, T) = c_v T + \frac{p_\infty}{\rho} + e_*, \tag{33}$$

$$\mu(\rho, T) = \gamma c_v T + e_* - c_v T \ln\Big(\frac{T}{T_0}\Big(\frac{\rho_0}{\rho}\Big)^{\gamma-1}\Big) - s_0 T, \tag{34}$$

where the ratio of specific heats is denoted by γ, the specific heat capacity at constant volume by c_v, and the zero point of energy by e_*. The reference temperature, density and entropy are denoted by T_0, ρ_0 and s_0, respectively. Finally, the parameter p_∞ has the effect of "stiffening" the phase, increasing the sound velocity. All these parameters are specific for each phase, which can be fitted using experimental data for a given fluid. Although the stiffened gas equation of state is one of the simplest EOSes available, it is nevertheless complex enough to allow modeling and simulation of a phase transfer process and even analytical expressions for most thermodynamic relations. As the main goal of this work is to demonstrate modeling of phase transfer, the limited range of validity of the stiffened gas EOS is not an important issue. If increased accuracy was required, one could replace the stiffened gas with a more complex EOS.

To write the flux function of the fluid mechanical equations (1)–(4) in terms of the conserved variables, i.e. the mass of each phase, the momentum and the total energy, all per unit volume, we need to express the pressure and temperature as functions of these variables. This may be accomplished using the procedure described by Flåtten, Morin, and Munkejord [30].

5. Numerical method

In order to numerically solve the two-phase flow model (1)–(4), we use a fractional-step method [31, Ch. 17]. In vector notation, the model can be written as

$$\frac{\partial \boldsymbol{q}}{\partial t} + \frac{\partial \boldsymbol{f}(\boldsymbol{q})}{\partial x} = \boldsymbol{s}(\boldsymbol{q}), \tag{35}$$

where $\boldsymbol{q} = [\alpha_g \rho_g, \alpha_\ell \rho_\ell, \rho v, E]^T$ is the vector of conserved variables, $\boldsymbol{f}$ is the flux function and $\boldsymbol{s}$ is the phase transfer source term.

We let Δt be the time step length and denote the numerical solution at $t^n = t_0 + n\,\Delta t$ by $\boldsymbol{q}^n$. In a simple first-order fractional-step method, often referred to as Godunov splitting, the numerical solution $\boldsymbol{q}^n$ is advanced in time using two steps:

1. Solve the hyperbolic conservation law
$$\frac{\partial \boldsymbol{q}}{\partial t} + \frac{\partial \boldsymbol{f}(\boldsymbol{q})}{\partial x} = 0 \tag{36}$$
in one time step yielding an intermediate solution $\boldsymbol{q}^*$.
2. Then solve the initial value problem
$$\frac{\partial \boldsymbol{q}}{\partial t} = \boldsymbol{s}(\boldsymbol{q}), \quad t \in [0, \Delta t], \quad \boldsymbol{q}(t=0) = \boldsymbol{q}^*, \tag{37}$$
yielding the solution $\boldsymbol{q}^{n+1}$.

The above scheme is first-order accurate in time as long as the numerical schemes used in each sub-step are at least first-order accurate.

One benefit of using a fractional-step method is that the composite problem is divided into sub-problems that are more easily solved by standard methods. The methods used in the sub-problems (36) and (37) are discussed below.

5.1. Hyperbolic part

The hyperbolic part of the fractional-step method (36) can be solved using a finite volume scheme, in which one divides the computational domain into control volumes. These numerical schemes ensures that the physically conserved variables are also conserved numerically. A finite volume scheme for Eq. (36) is obtained by integrating over a control volume, which yields

$$\frac{\mathrm{d}\boldsymbol{Q}_i}{\mathrm{d}t} = -\frac{1}{\Delta x}(\boldsymbol{F}_{i+1/2} - \boldsymbol{F}_{i-1/2}), \tag{38}$$

where $\boldsymbol{Q}_i$ is the average of $\boldsymbol{q}$ in control volume i, and $\boldsymbol{F}_{i+1/2}$ is the numerical flux between control volume i and $i+1$. Eq. (38) is an ODE which can be solved using e.g. the forward Euler or higher-order Runge-Kutta time-stepping methods. At each cell interface, there is a discontinuity in $\boldsymbol{Q}$ at each time step t^n, and finding the solution for later times ($t > t^n$) is commonly referred to as a Riemann problem.

The multi-stage (MUSTA) approach was first suggested by Toro [32], Titarev and Toro [33], and is based on solving the Riemann problem using a first-order centred scheme on a *local* grid at each cell interface. The solution from the local grid is then used to find the flux in the *global* grid. An advantage with the MUSTA scheme, compared to other Riemann solvers, is that it is relatively simple. We will use the MUSTA 2–2 scheme investigated by Munkejord, Evje, and Flåtten [34] for solving the phase transfer model (1)–(4) and the equilibrium model (9).

To achieve a higher-order method, one can employ the monotone upwind-centred scheme for conservation laws (MUSCL) (see e.g. van Leer [35], Osher [36]), which is based on making a piecewise linear reconstruction using the data $\{\boldsymbol{Q}_i\}$. The allowable slope in each cell is determined by a *slope-limiter* function, of which there are many possible choices. We choose the minmod limiter, which was demonstrated as a good choice by Munkejord, Evje, and Flåtten [34].

5.2. Relaxation ODE

The initial value problem (37) can in principle be solved by a large number of schemes for solving ODEs. In this work we use the first-order backward Euler scheme, given by

$$\boldsymbol{q}^{n+1} = \boldsymbol{q}^{*} + \boldsymbol{s}(\boldsymbol{q}^{n+1})\,\Delta t. \tag{39}$$

The implicit scheme ensures a stable and robust numerical solution, even for stiff problems. The nonlinear equation system (39) was solved using the Newton-Raphson method.

6. Simulation results

In this section, we will present results from simulation of a depressurisation of a pipe of length $L = 80$ m with pure CO_2. As the initial condition at time $t = 0$ s, we have liquid at $p_{0,\mathrm{L}} = 60$ bar in the left ($x < 50$ m) part of the pipe, and gas at $p_{0,\mathrm{L}} = 10$ bar in the right ($x > 50$ m) part. The temperature is $T_0 = 273$ K ≈ 0 °C, and the fluid is stationary ($v_0 = 0$ m/s). The temperature and pressure at each end is kept constant throughout the simulation. The stiffened gas parameters used are presented in Table 1.

Table 1: Stiffened gas parameters

Phase	γ (dimensionless)	p_∞ (Pa)	c_v (J/kg K)	e_* (J/kg)	s_0 (J/kg K)	ρ_0 (kg/m^3)	T_0 (K)
Gas	1.06	$8.86 \cdot 10^5$	$2.41 \cdot 10^3$	$-3.01 \cdot 10^5$	$1.78 \cdot 10^3$	135	283.13
Liquid	1.23	$1.32 \cdot 10^8$	$2.44 \cdot 10^3$	$-6.23 \cdot 10^5$	$1.09 \cdot 10^3$	861	283.13

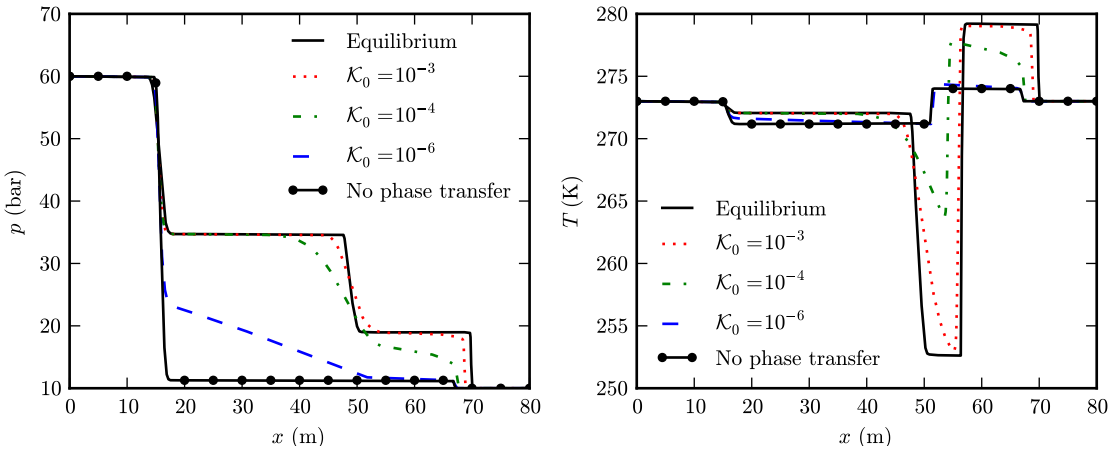

(a) Pressure (b) Temperature

Fig. 1: Simple model, time $t = 0.08$ s. 4000 (solid lines) or 2000 (dotted/dashed lines) cells. CFL number = 0.5.

As time progresses, a rarefaction (decompression) wave will propagate leftward from $x = 50$ m, and a shock wave will propagate to the right. Figure 1 shows the results at time $t = 0.08$ s using the simple model (10), together with those of the equilibrium model (9). As expected, the value of the rate constant $\mathcal{K}_0$ is crucial to the behaviour of the system. Compared to the equilibrium model, the phase transfer model smoothens the solution, approaching the model without phase transfer as $\mathcal{K}_0 \to 0$. Having no information about the physically correct value of $\mathcal{K}_0$, this model offers little in predicting the behaviour of the actual physical system.

In Figure 2, the results at time $t = 0.08$ s for the SRT model are shown. The results are quite similar when changing the initial volume fraction δ, and are quite close to those of the equilibrium model. We note a

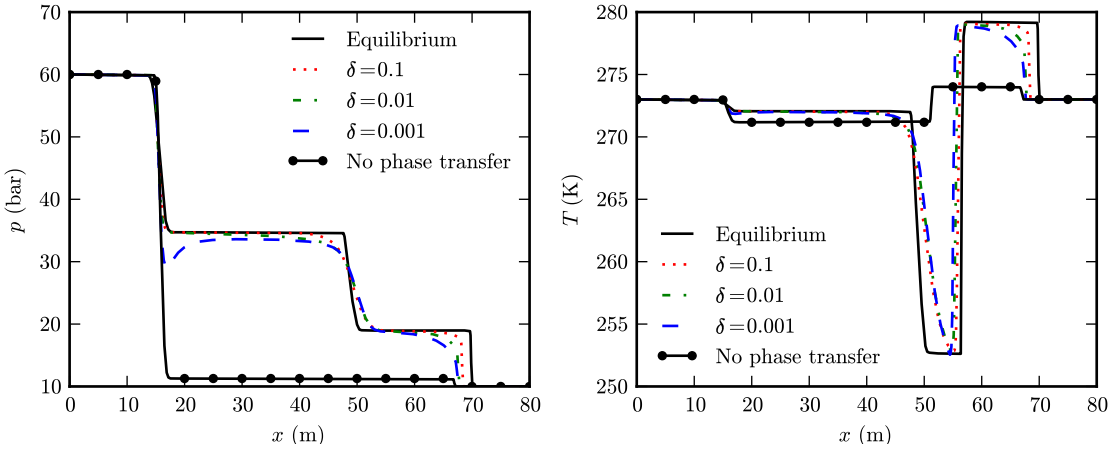

(a) Pressure (b) Temperature

Fig. 2: SRT model, time $t = 0.08$ s. 4000 (solid lines) or 2000 (dotted/dashed lines) cells. CFL number = 0.5.

small dip in the solution for $\delta = 0.001$ at $x \approx 18$ m, which is where the border between the one-phase liquid region and the two-phase region is located. This can explain the dip, since a small initial volume fraction δ will cause a slower start-up of the evaporation. Further to the right ($x > 25$ m) into the two-phase region, we see that the dependence on δ is less pronounced, since we are past the start-up phase in this region.

As with the simple model (10), the discontinuities are smoothened quite a bit compared to the equilibrium model. We remind the reader that the interfacial area used is a lower approximation of what the actual area is. With a larger area, the phase transfer would be more rapid, and the results even closer to the equilibrium model. Hence, our results indicate that pressure and temperature during a depressurisation would be quite close to those of an equilibrium model. However, our model with phase transfer modeled using SRT avoids potential problems caused by discontinuous speed of sound in the equilibrium model, and is also able to capture the dynamics of the phase transfer process in situations where this is crucial.

7. Conclusion

We have presented two phase transfer models: a simple model and a model developed based on statistical rate theory (SRT) capable of describing evaporation and condensation of CO_2. These were combined with a two-phase drift-flux flow model to yield a framework for simulating flow in a pipeline with a two-phase CO_2 mixture. We have presented simulation results for a depressurisation of a pipeline, where the SRT model was used to predict phase transfer in a two-phase mixture flow, and which showed qualitatively very similar behaviour to the equilibrium model. Future comparison with experiments with either water or carbon dioxide will be interesting to validate the model.

Acknowledgement

This work was financed through the CO2 Dynamics project. The authors acknowledge the support from the Research Council of Norway (189978), Gassco AS, Statoil Petroleum AS and Vattenfall AB.

References

[1] OECD/IEA, Energy Technology Perspectives 2010, 2010.
[2] T. Flåtten, H. Lund, Relaxation Two-Phase Flow Models and the Subcharacteristic Condition, Mathematical Models and Methods in Applied Sciences 21 (12) (2011) 1–29.

[3] T. Flåtten, A. Morin, S. T. Munkejord, Wave propagation in multicomponent flow models, SIAM Journal on Applied Mathematics 70 (8) (2010) 2861–2882.
[4] H. Lund, T. Flåtten, S. T. Munkejord, Depressurization of Carbon Dioxide in Pipelines - Models and Methods, Energy Procedia 4 (2011) 2984–2991.
[5] C. A. Ward, G. Fang, Expression for predicting liquid evaporation flux: Statistical rate theory approach, Phys. Rev. E 59 (1) (1999) 429–440, doi:10.1103/PhysRevE.59.429.
[6] Y.-P. Pao, Application of Kinetic Theory to the Problem of Evaporation and Condensation, Physics of Fluids 14 (2) (1971) 306–312, doi:10.1063/1.1693429, URL http://link.aip.org/link/?PFL/14/306/1.
[7] L. D. Koffman, M. S. Plesset, L. Lees, Theory of evaporation and condensation, Physics of Fluids 27 (4) (1984) 876–880, doi:10.1063/1.864716, URL http://link.aip.org/link/?PFL/27/876/1.
[8] P. Rahimi, C. A. Ward, Kinetics of Evaporation: Statistical Rate Theory Approach, Int. J. of Thermodynamics 8 (2005) 1–14.
[9] C. A. Ward, The rate of gas absorption at a liquid interface, The Journal of Chemical Physics 67 (1) (1977) 229–235, doi: 10.1063/1.434547, URL http://link.aip.org/link/?JCP/67/229/1.
[10] C. A. Ward, R. D. Findlay, M. Rizk, Statistical rate theory of interfacial transport. I. Theoretical development, The Journal of Chemical Physics 76 (11) (1982) 5599–5605, doi:10.1063/1.442865, URL http://link.aip.org/link/?JCP/76/5599/1.
[11] M. Dejmek, C. A. Ward, A statistical rate theory study of interface concentration during crystal growth or dissolution, The Journal of Chemical Physics 108 (20) (1998) 8698–8704, doi:10.1063/1.476298, URL http://link.aip.org/link/?JCP/108/8698/1.
[12] S. Azizian, H. Bashiri, H. Iloukhani, Statistical Rate Theory Approach to Kinetics of Competitive Adsorption at the Solid/Solution Interface, Journal of Physical Chemistry C 112 (27) (2008) 10251–10255, doi:10.1021/jp802278e, URL http://pubs.acs.org/doi/abs/10.1021/jp802278e.
[13] W. Rudzinski, W. Plazinski, Kinetics of solute adsorption at solid/solution interfaces: A theoretical development of the empirical pseudo-first and pseudo-second order kinetic rate equations, based on applying the statistical rate theory of interfacial transport, Journal of Physical Chemistry B 110 (33) (2006) 16514–16525, ISSN 1520-6106, doi:10.1021/jp061779n.
[14] J. A. W. Elliott, C. A. Ward, Statistical rate theory description of beam-dosing adsorption kinetics, Journal of Chemical Physics 106 (13) (1997) 5667–5676, ISSN 0021-9606.
[15] R. D. Findlay, C. A. Ward, Statistical Rate Theory of Interfacial Transport. IV. Predicted Rate of Dissociative Adsorption, Journal of Chemical Physics 76 (11) (1982) 5624–5631, ISSN 0021-9606.
[16] J. A. W. Elliott, C. A. Ward, Temperature programmed desorption: A statistical rate theory approach, The Journal of Chemical Physics 106 (13) (1997) 5677–5684, doi:10.1063/1.473588, URL http://link.aip.org/link/?JCP/106/5677/1.
[17] F. Bordi, C. Cametti, A. Motta, Ion Permeation Across Model Lipid Membranes: A Kinetic Approach, The Journal of Physical Chemistry B 104 (22) (2000) 5318–5323, doi:10.1021/jp000005i, URL http://pubs.acs.org/doi/abs/10.1021/jp000005i.
[18] L. B. Harding, A. I. Maergoiz, J. Troe, V. G. Ushakov, Statistical rate theory for the HO + O ⇔ HO_2 ⇔ H + O_2 reaction system: SACM/CT calculations between 0 and 5000 K, Journal of Chemical Physics 113 (24) (2000) 11019–11034, ISSN 0021-9606.
[19] A. Kapoor, J. A. W. Elliott, Nonideal Statistical Rate Theory Formulation To Predict Evaporation Rates from Equations of State, Journal of Physical Chemistry B 112 (47) (2008) 15005–15013, ISSN 1520-6106, doi:10.1021/jp804982g.
[20] C. A. Ward, D. Stanga, Interfacial conditions during evaporation or condensation of water., Phys Rev E 64 (2001) 051509, ISSN 1539-3755.
[21] M. Bond, Non-Equilibrium Evaporation and Condensation, Master's thesis, University of Victoria, 2004.
[22] R. Saurel, F. Petitpas, R. Abgrall, Modelling phase transition in metastable liquids: application to cavitating and flashing flows, Journal of Fluid Mechanics 607 (2008) 313–350.
[23] H. B. Stewart, B. Wendroff, Two-phase flow: Models and methods, Journal of Computational Physics 56 (1984) 363–409.
[24] D. Bestion, The physical closure laws in the CATHARE code, Nuclear Engineering and Design 124 (1990) 229–245.
[25] M.-S. Chung, K.-S. Chang, S.-J. Lee, Wave propagation in two-phase flow based on a new hyperbolic two-fluid model, Numerical Heat Transfer, Part A 38 (2000) 169–191.
[26] J. Cortes, On the construction of upwind schemes for non-equilibrium transient two-phase flows, Computers & Fluids 31 (2002) 159–182.
[27] I. Toumi, An upwind numerical method for two-fluid two-phase flow models, Nuclear Science and Engineering 123 (1996) 147–168.
[28] R. Menikoff, B. J. Plohr, The Riemann problem for fluid flow of real materials, Rev. Mod. Phys. 61 (1989) 75–130.
[29] R. Menikoff, Empirical equations of state for Solids, Shock Wave Science and Technology Reference Library 2 (2007) 143–188.
[30] T. Flåtten, A. Morin, S. T. Munkejord, On the solution of equilibrium problems for systems of stiffened gases, SIAM Journal on Applied Mathematics 71 (1) (2011) 41–67.
[31] R. J. LeVeque, Finite Volume Methods for Hyperbolic Problems, Cambridge University Press, 2002.
[32] E. F. Toro, Multi-stage predictor-corrector fluxes for hyperbolic equations, Technical Report NI03037-NPA, Isaac Newton Institute for Mathematical Sciences, University of Cambridge, UK, 2003.
[33] V. A. Titarev, E. F. Toro, MUSTA schemes for multi-dimensional hyperbolic systems: analysis and improvements, International Journal for Numerical Methods in Fluids 49 (2005) 117–147.
[34] S. T. Munkejord, S. Evje, T. Flåtten, The multi-stage centred-scheme approach applied to a drift-flux two-phase flow model, International Journal for Numerical Methods in Fluids 52 (6) (2006) 679–705.
[35] B. van Leer, Towards the ultimate conservative difference scheme V. A second order sequel to Godunov's method, Journal of Computational Physics 32 (1) (1979) 101–136.
[36] S. Osher, Convergence of generalized MUSCL schemes, SIAM Journal on Numerical Analysis 22 (5) (1985) 947–961.